Synthesis, Structure and Oxidation of $[NiL^1]^{2+}$ [L^1 = 5-(4-amino-2-azabutyl)-5-methyl-3,7-diazanonane-1,9-diamine]: Evidence for Rearrangement within the Complexed Nickel(III) Species *

Alexander McAuley,[a] Seth Subramanian[b] and Todd W. Whitcombe[a]
[a] *Department of Chemistry, Universityof Victoria, Victoria B.C., V8W 3P6, Canada*
[b] *Department of Chemistry, St. Mary's University, Halifax, Nova Scotia, Canada*

The ligand 5-(4-amino-2-azabutyl)-5-methyl-3,7-diazanonane-1,9-diamine, L^1, has been synthesised and a nickel(II) complex, $[NiL^1]Br_2$, characterized by X-ray crystallography (monoclinic, space group $P2_1/n$, a = 14.143, b = 9.618, c = 13.552, β = 106.14°, Z = 4, R = 0.0429, R' = 0.0418). The cation adopts a distorted octahedral geometry typical of similar nickel(II) complexes. The complex $[NiL^1]^{2+}$ can be oxidized, under neutral conditions, either electrochemically or by use of $S_2O_8^{2-}$ to a moderately stable nickel(III) complex. By monitoring the reaction with $S_2O_8^{2-}$ using ESR spectroscopy, evidence has been obtained for three species, with characteristic ESR signals, g_1, g_2 and g_3. These represent the initial nickel(III) complexed ion and two structural modifications formed through substitution by sulfate. The final product is a distorted tetragonal complex with axial sulfate ligation. These reactions represent a rare example of ligand substitution at an NiN_6^{3+} chromophore. A second-order rate constant of 0.26 ± 0.05 dm^3 mol^{-1} s^{-1} for the reaction of $[NiL^1]^{2+}$ with $S_2O_8^{2-}$ has been obtained.

An ongoing theme in macrocyclic chemistry, giving rise to a cryptic geometry,[1-4] is the encapsulation of a metal centre within a ligating framework. A consequence of this co-ordination is that the metal ion may exhibit properties different from those that might be ascribed to it in a less encapsulating environment. The attainment of both low and high unusual oxidation states may be achieved or the substitution properties of a metal ion may be altered considerably.

The formation of nickel(III) ions in solution is predominantly the preserve of macrocyclic complexes. Few examples exist wherein an identifiable nickel(III) centre exists in an open-chain ligand.[5] With the exception of the amide complexes,[5] most non-macrocyclic systems have been studied by pulse radiolysis techniques.[6] However, for kinetic stability, the ligand should contain sufficient co-ordination sites to satisfy completely the octahedral requirements of the metal centre. With the theme of encapsulating a metal ion within a simple ligand framework and examining its redox properties, the ligand 5-(4-amino-2-azabutyl)-5-methyl-3,7-diazanonane-1,9-diamine (L^1) has been synthesised by a modification of established procedures.[7] This ligand co-ordinates as a hemisarcophogane. An analogous complex with an axial ethyl replacing the methyl group has been synthesised by Green *et al.*[7] These workers examined the stability constants of the copper(II), nickel(II) and cobalt(II) complexes but encountered multinuclear complexes in addition to the simple 1 : 1 adducts. Cobalt(III) complexes of L^1 were first reported by Sarneski and Urbach,[8] who examined their stereochemistry. Tomioka *et al.*[9] developed a 'rational' synthesis to the ligand utilizing 1,1,1-tris(toluene-*p*-sulfonyloxymethyl)-ethane and ethylenediamine (en). The products were identified, by analysis of their cobalt complexes, as two structurally different ligands, one of which was L^1. Subsequently, Geue and Searle[10] devised a procedure to isolate the cobalt complex of L^1 selectively. In the present paper, we report the synthesis and structure of the $[NiL^1]^{2+}$ ion and examine its redox properties in aqueous solution.

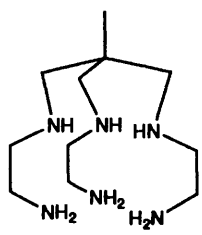

L^1

Experimental

All chemicals used were of reagent or spectroscopic grades unless otherwise specified.

Preparation of 5-(4-*Amino*-2-*azabutyl*)-5-*methyl*-3,7-*diazanonane*-1,9-*diamine* L^1.—1,1,1-Tris(bromomethyl)ethane (34.0 g, 0.11 mol) was refluxed at 140–150 °C with anhydrous ethylenediamine (500 cm^3, 8.5 mol) in a moisture- and CO_2-free atmosphere for 72 h. The reaction mixture was cooled and the excess of ethylenediamine was removed using a rotary evaporator. The resulting viscous oil weighed 73.5 g. This material was dissolved in water (500 cm^3) and adsorbed on a Dowex 50X8 ion-exchange resin column. Washing with 2.0 mol dm^{-3} HCl (6 dm^3) removed any residual ethylenediamine. The column was subsequently washed with 4.0 mol dm^{-3} HCl (6 dm^3) and the eluent collected was concentrated to 200 cm^3. Addition of ethanol (500 cm^3) to the concentrate, with stirring at 60 °C, led to the deposition of a white crystalline powder (46 g, 90% yield) which was identified as the hydrochloride salt of L^1 containing trace impurities. A small amount of the free amine was obtained by neutralizing the L^1·6HCl with 40% NaOH and extracting the liberated amine with pyridine. The

* *Supplementary data available:* see Instructions for Authors, *J. Chem. Soc., Dalton Trans.*, 1993, Issue 1, pp. xxiii–xxviii.

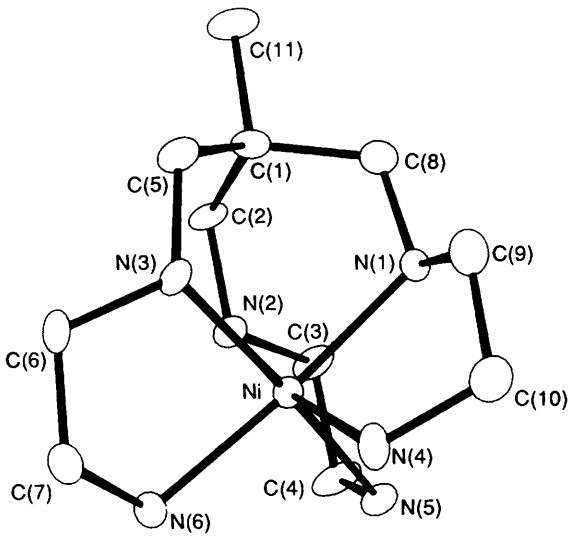

Fig. 1 An ORTEP[15] diagram of $[NiL^1]^{2+}$ showing the atomic labelling scheme. Hydrogen atoms are omitted for clarity

extract was dried over KOH and concentrated to give a colourless hydroscopic oil. The molecular weight of the amine was confirmed by chemical ionization (CI) mass spectroscopy (M + 1 247). ^{13}C NMR of L^1·6HCl in D_2O: δ 20.9 (q, CH_3), 39.2 (s, quaternary C), 55.5 (t, CCH_2NH), 48.9 (t, $-NHCH_2-CH_2NH_2$) and 38.5 (t, CH_2NH_2).

Preparation of $[NiL^1][ClO_4]_2$.—**CAUTION**: Metal perchlorate salts are hazardous and should be treated with caution. The crude ligand hydrochloride (4.7 g, 0.01 mol) was dissolved in water (50 cm^3) and a solution of nickel(II) acetate (2.5 g, 0.01 mol) in water (10 cm^3) was added. The resulting mixture was warmed in a beaker on a hot plate while solid sodium carbonate was added until no effervescence was observed and the pH was approximately 7. A small portion of the reaction mixture was separated using a Sephadex C-25 SP cation exchange column yielding a single major band with only traces of intractable impurities. The remaining reaction mixture was saturated with sodium perchlorate precipitating the pink perchlorate salt which was filtered off and air dried (4.2 g, 84% yield). Recrystallization from boiling water in the presence of sodium perchlorate gave analytically pure crystals (Found: C, 26.20; H, 5.95; Cl, 13.90; N, 16.50, Ni, 11.40; O, 25.20. $C_{11}H_{30}Cl_2N_6NiO_8$ requires C, 26.20; H, 6.00; Cl, 14.10; N, 16.70; Ni, 11.65; O, 25.40%).

Preparation of $[NiL^1]Br_2$.—The crude perchlorate salt was dissolved in a minimum of water and adsorbed on a Sephadex C-25 SP cation exchange column and eluted with 0.1–0.2 mol dm^{-3} NaCl. The first trace pink band was discarded. The second (major) band was collected and concentrated to near dryness. The resulting solution was extracted with propan-2-ol to remove the excess of NaCl. To the propan-2-ol fraction, a saturated solution of sodium bromide in water was added. The resulting precipitate was further recrystallized from water containing sodium bromide to provide single crystals suitable for X-ray crystallography (Found: C, 27.90; H, 6.45; N, 17.65; Ni, 12.40. $C_{11}H_{30}Br_2N_6Ni$ requires C, 27.90; H, 6.45; N, 17.75; Ni, 12.90%).

Crystallography.—The purple crystal was mounted inside a Lindemann tube using epoxy resin and aligned by Weissenberg and precession photography, which yielded a preliminary unit cell and space group. The crystal was transferred to a Picker four-circle diffractometer connected to a PDP-11 computer and the unit cell was refined using 19 pairs of reflections in the range $22 < 2\theta < 50°$. Data were collected in 200 steps of 0.25 s with 25 s of background counting before and after each peak.

The phase problem was solved using the direct methods package of SHELX 76.[11] After application of an absorption correction,[12] least-squares refinement of the structure yielded a final value of $R = 0.0429$ ($R' = 0.0418$) with all non-hydrogen atoms defined anisotropically. The hydrogen atoms were obtained from the difference maps and were included in the final stages of refinement with a common isotropic thermal parameter. The atomic scattering factors together with the Ni f-curve were taken from the usual source.[13] The maximum residual electron density was ≈0.8 e $Å^{-3}$ located near the bromide ion (< 1 Å). A maximum shift/estimated standard deviation of 0.008 was obtained in the final cycle.

Additional material available from the Cambridge Crystallographic Data Centre comprises H-atom coordinates, thermal parameters and remaining bond lengths and angles.

Spectroscopy.—Proton and ^{13}C NMR spectra were obtained on a Bruker WM250 spectrometer, ESR spectra using a Varian E6S instrument fitted with either a liquid-nitrogen insert Dewar or a quartz flat cell. Stopped-flow ESR measurements were made using a locally constructed system which adapted a flat cell with a mixing chamber. UV/VIS spectroscopy was performed on either a Perkin Elmer Lambda 4B or a Cary 5 spectrometer using quartz cells. Electrochemical measurements were obtained using a PAR 273 Galvanostat/Potentiostat equipped with an IBM PC running HEADSTART (Princeton Applied Research). Normal three-electrode cells employing platinum working and counter electrodes and an appropriate reference electrode were employed. Potentials quoted are relative to the normal hydrogen electrode (NHE), unless otherwise stipulated. Stopped-flow measurements were made with an Applied Photophysics DX-17MV spectrometer equipped with an Acorn computer.

All aqueous solutions utilized in physical measurements were prepared from doubly distilled water which was treated in a Barnstead HN Ultrapure mixed bed column. The $K_2S_2O_8$ used in the kinetic experiments was recrystallized multiple times (> 7) prior to use. In our experience, with material from fewer recrystallizations inconsistent and less reproducible data were derived. In all cases where feasible, fresh solutions of $K_2S_2O_8$ were made just prior to the experiment.

Results and Discussion

Synthesis.—The synthesis of the ligand 5-(4-amino-2-azabutyl)-5-methyl-3,7-diazanonane-1,9-diamine (L^1) is part of an overall scheme for the generation of open-chained and macrocyclic compounds centred around a C-spiro carbon.[14] However, the ligand also represents a close analogue of the cryptate ligands explored by Sargeson and co-workers.[2] While the synthesis of the ligand may be carried out in relatively good yields, its recovery and purification is enhanced by utilizing metal ions to provide a charged complex ion that is readily separated by column chromatography. The nickel(II) complex may be obtained readily and recrystallization affords X-ray quality crystals.

Crystallography.—The crystal structure of $[NiL^1]Br_2$ is shown in Fig. 1, together with the atomic labelling scheme for all non-hydrogen atoms. The hydrogen atoms have been omitted for clarity of presentation. Pertinent crystallographic data are contained in Table 1, while the fractional coordinates, selected bond lengths and bond angles are presented in Tables 2 and 3.

The nickel atom is not located on a symmetry element and hence the whole molecule constitutes the asymmetric unit which suggests an absence of rigorous symmetry in the solid state. This can be contrasted with the structurally similar cations $[NiL^2]^{2+}$ (L^2 = 1,3,6,8,10,13,16,19-octaazabicyclo-

Table 1 Crystallographic parameters for $[NiL^1]Br_2$

Formula	$C_{11}H_{30}Br_2N_6Ni$
M	464.92
Crystal symmetry	Monoclinic
Space group	$P2_1/n$
a/Å	14.143(6)
b/Å	9.618(3)
c/Å	13.552(6)
β/°	106.14(3)
U/Å^3	1770.8(12)
Z	4
D_c/g cm^{-3}	1.744
Radiation (λ/Å)	Mo-Kα (0.710 69)
2θ/°	0.1–50.0
Number of reflections	3121
Number of observed reflections [$I > \sigma(I)$]	2646
Number of parameters	272
Maximum residual electron density/e Å^{-3}	0.8
Maximum final shift/e.s.d.	0.008
μ/cm^{-1}	55.73
R,[a] R'[b]	0.0429, 0.0418

[a] $R = \Sigma(|F_o| - |F_c|)/\Sigma|F_o|$. [b] $R' = [\Sigma(|F_o| - |F_c|)^2/\Sigma w(|F_o|)^2]^{\frac{1}{2}}$ where $w = 1.0/[\sigma^2(F) + 0.0005F^2]$.

Table 2 Fractional atomic coordinates ($\times 10^5$ for Ni and Br, $\times 10^4$ for C and N) for non-hydrogen atoms of $[NiL^1]Br_2$ with estimated standard deviations (e.s.d.s) in parentheses

Atom	X/a	Y/b	Z/c
Ni	46 768(4)	70 010(6)	24 495(4)
Br(1)	13 867(4)	80 995(6)	9 561(4)
Br(2)	83 308(4)	19 322(7)	47 233(4)
N(1)	4 703(3)	8 312(4)	3 708(3)
N(2)	6 056(3)	7 773(4)	2 417(3)
N(3)	4 000(3)	8 623(4)	1 450(3)
N(4)	3 353(3)	6 279(5)	2 695(4)
N(5)	5 544(4)	5 439(5)	3 391(4)
N(6)	4 515(3)	5 908(5)	1 050(3)
C(1)	5 309(4)	10 119(5)	2 659(4)
C(2)	5 146(4)	9 704(5)	3 686(4)
C(3)	3 656(4)	8 374(6)	3 742(5)
C(4)	3 246(4)	6 928(6)	3 651(5)
C(5)	6 168(4)	9 310(5)	2 436(5)
C(6)	6 805(4)	7 048(6)	3 228(4)
C(7)	6 539(4)	5 527(6)	3 228(5)
C(8)	4 359(4)	10 041(5)	1 782(5)
C(9)	4 091(4)	8 249(6)	420(4)
C(10)	3 872(4)	6 743(7)	232(4)
C(11)	5 610(5)	11 672(6)	2 751(6)

Table 3 Selected bond lengths (Å) and angles (°) for $[NiL^1]Br_2$ with e.s.d.s in parentheses

N(1)–Ni	2.112(4)	C(9)–N(3)	1.481(6)
N(2)–Ni	2.099(4)	C(4)–N(4)	1.483(7)
N(3)–Ni	2.113(4)	C(7)–N(5)	1.487(7)
N(4)–Ni	2.109(4)	C(10)–N(6)	1.463(7)
N(5)–Ni	2.126(5)	C(2)–C(1)	1.525(7)
N(6)–Ni	2.124(4)	C(5)–C(1)	1.542(6)
C(2)–N(1)	1.482(6)	C(8)–C(1)	1.529(7)
C(3)–N(1)	1.495(6)	C(11)–C(1)	1.549(7)
C(5)–N(2)	1.487(6)	C(4)–C(3)	1.499(7)
C(6)–N(2)	1.472(6)	C(7)–C(6)	1.510(8)
C(8)–N(3)	1.481(6)	C(10)–C(9)	1.488(8)
N(2)–Ni–N(1)	89.9(1)	N(5)–Ni–N(3)	171.8(2)
N(3)–Ni–N(1)	88.8(2)	N(5)–Ni–N(4)	93.6(2)
N(3)–Ni–N(2)	89.1(1)	N(6)–Ni–N(1)	171.6(2)
N(4)–Ni–N(1)	83.5(2)	N(6)–Ni–N(2)	91.5(2)
N(4)–Ni–N(2)	172.3(2)	N(6)–Ni–N(3)	82.9(2)
N(4)–Ni–N(3)	94.6(2)	N(6)–Ni–N(4)	95.6(2)
N(5)–Ni–N(1)	93.4(2)	N(6)–Ni–N(5)	95.0(2)
N(5)–Ni–N(2)	83.0(2)		

[6.6.6]eicosane)[1] and $[NiL^3]^{2+}$ (L^3 = 3,6,10,13,16,19-hexaazabicyclo[6.6.6]eicosane-1,8-diamine),[2d] both of which demonstrate symmetry axes within the crystalline state (three-fold in the former and two-fold in the latter). Since the major structural differences between $[NiL^1]^{2+}$, $[NiL^2]^{2+}$ and $[NiL^4]^{2+}$ (L^4 = 3,6,10,13,16,19-hexaazabicyclo[6.6.6] eicosane) is the capping of only one end *versus* both ends of the ethylenediamine-like core, the freedom of movement or the disposition of the primary amines must be of fundamental importance to the overall structural geometry of the complex ion. This is reflected further in the distribution of the amines within the primary co-ordination sphere where a 'tetragonal' shortening is observed along the axis described by N(2)–Ni–N(4). For the primary amine nitrogen, N(4), a bond length of 2.109 Å is obtained which is 0.016 Å shorter than the comparable bonds to N(6) and N(5) (2.124, 2.126 Å). For the secondary amine nitrogen, N(2), the bond length of 2.099 Å is 0.013 Å shorter than the remaining Ni–N bonds (2.122, 2.113 Å). However, the mean planes describing the two sets of nitrogen donors (primary and secondary) are essentially parallel to each other (1.5°) which provides a picture of the primary co-ordination geometry as a distorted octahedron resulting from a slight displacement of the two opposing trigonal faces.

It can also be seen that the average inter-nitrogen distance for the primary amines is 0.15 Å greater than for the secondary amines. This is in keeping with the anticipated structural rigidity of the apical cap as well as the relative bond strengths of the Ni–N bonds. The geometry and bond lengths within the four carbon atoms of the capping group confine the secondary amines to their relative positions. Similar distortions have been observed in other 'capped' complexes.[2,16,17]

Of interest in this compound is the twist angle for the N_3 planes as viewed down the putative molecular C_3 axis. This angle has been correlated with apparent ligand-field stabilization energy for a series of caged metal ion complexes.[17] In the present case, an angle of 51.5° may be calculated which is slightly larger than that observed for $[NiL^2]^{2+}$ (48.0°) and $[Ni(H_2L^3)]^{4+}$ (47.1°) but close to the value for $[Ni(en)_3]^{2+}$ (≈50.5°). The relative similarity of the twist angle in these analogous complexes suggests that the major driving force for the disposition of the ligand resides in the electronic demands of the metal centre and that structural differences reflect the ability of the ligands to accommodate these demands. With the cryptands, the free ligand has an intrinsic twist angle of ≈24°[17] and thus is distorted to achieve the co-ordination complex.

Electrochemistry.—The $[NiL^1]^{2+}$ complex is electrochemically active generating a nickel(III) species in aqueous media. The redox couple gives a reversible cyclic voltammogram in 0.1 mol dm^{-3} $LiNO_3$ with $E_{\frac{1}{2}}$ = 700 mV *vs.* saturated calomel electrode (SCE) (0.923 V *vs.* NHE; ΔE_p = 60 mV; $i_a/i_c \approx 0.90$). A decrease of 70 mV is observed in $E_{\frac{1}{2}}$ when 3.56 mol dm^{-3} LiCl is used as supporting electrolyte while the peak retains its reversible characteristics. A shift of this magnitude, relative to the change in overall ionic strength and the nature of the anion, is more indicative of the formation of an ion pair than of complexation by the chloride ion.

The kinetic studies (see below) provide evidence for the slow conversion of the nickel(III) complex generated initially to other forms but the time span involved in the cyclic voltammogram and the shape and ΔE of the observed wave are in keeping with a simple oxidation of $[NiL^1]^{2+}$ to $[NiL^1]^{3+}$. The redox potential of 0.923 V *vs.* NHE for $[NiL^1]^{2+/3+}$ is very close to those of other Ni^{2+}–Ni^{3+} couples such as $[NiL^5_2]^{2+/3+}$ (L^5 = 1,4,7-triazacyclononane) (0.947 V),[18] $[NiL^4]^{2+/3+}$ (0.90)[2d] and $[NiL^6]^{2+/3+}$ (L^6 = 1,4,8,11-tetraazacyclotetradecane) (0.97)[19] further suggesting a commonality of structure and reactivity.

Table 4 UV/VIS spectroscopic parameters for NiN_6 chromophores

Complex	Transitions, λ_{max}/nm (ε/dm^3 mol^{-1} cm^{-1}) $^3T_{1g}(P) \longleftarrow {}^3A_{2g}$	$^3T_{1g}(F) \longleftarrow {}^3A_{2g}$	Ref.
$[Ni(en)_3]^{2+}$	345 (9.0)	545 (6.9)	1
$[NiL^1]^{2+}$	326 (9.8)	523 (7.6)	This work
$[Ni(Htam)_2]^{4+}$	331 (8.5)	519 (6.9)	16
$[NiL^2]^{2+}$	316 (11.2)	510 (8.0)	1
$[NiL^4]^{2+}$	329 (9.2)	506 (8.8)	2(*d*)
$[NiL^5{}_2]^{2+}$	322 (11.0)	504 (11.0)	18

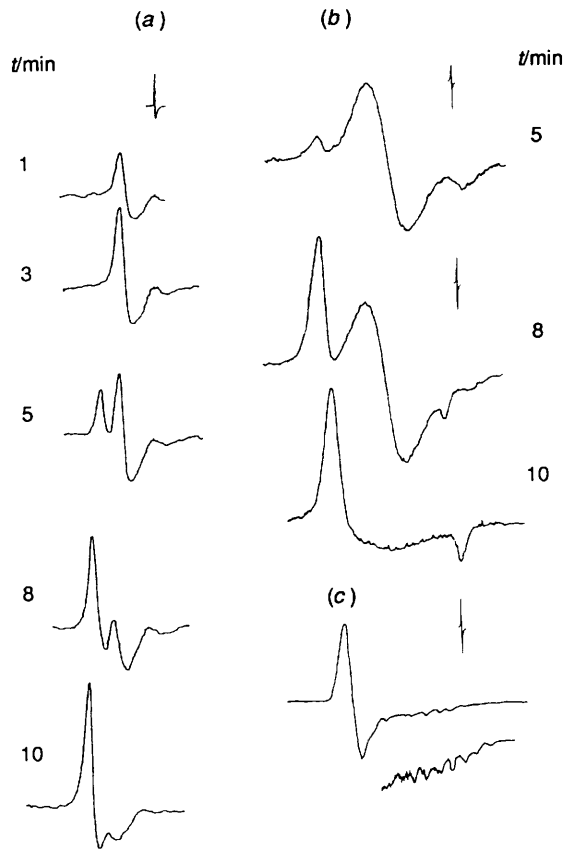

Fig. 2 Flat-cell (*a*) and low-temperature (*b*) ESR spectra of the $[NiL^1]^{3+}$ complex generated using $S_2O_8^{2-}$. The spectra clearly indicate the conversion of the nickel(III) species formed initially to a second species. The low-temperature spectrum obtained in the presence of chloride (*c*) exhibits superhyperfine coupling for its axial component

UV/VIS Spectroscopy.—The UV/VIS spectra of the nickel-(II) and -(III) complexes were studied in aqueous media. The spectrum for $[NiL^1]^{2+}$ is typical on a NiN_6 chromophore exhibiting two bands (Table 4). Both the perchlorate and bromide salts exhibit identical spectroscopic features. Neither the addition of potentially complexing anions nor variations in temperature produced any changes in the spectra, confirming the structural integrity of the complex in solution.

Comparison with other NiN_6^{2+} complexes demonstrates the effects of structural variation on the energies for the two transitions. A progression in the magnitude of the crystal field splitting for $[Ni(en)_3]^{2+}$ (no caps), $[NiL^1]^{2+}$ (1 cap) and $[NiL^4]^{2+}$ and $[NiL^2]^{2+}$ (2 caps) can be observed in Table 4. The capping of the N_6 chromophore endows a stronger ligand field in comparison to the 'open' complexes as might be anticipated. An interesting comparison is also provided by $[Ni(Htam)_2]^{4+}$ [tam = tetra(aminomethyl)methane] which

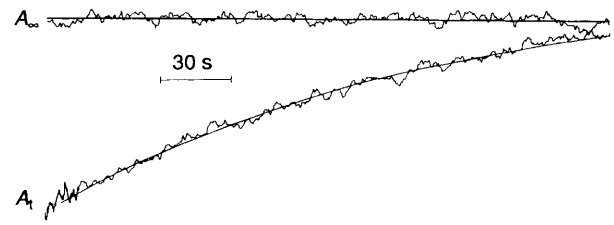

Fig. 3 Stopped-flow ESR trace obtained for the initial formation of the nickel(III) species. The solid lines represent the decay in peak intensity (A_t) and the infinity value (A_∞) used to calculate a rate constant of 10.4×10^{-3} s^{-1} for the formation of $[NiL^1]^{3+}$

co-ordinates as essentially two caps and no sides but where a similar ligand field is observed.[16] However, the overall trends are in keeping with the relative importance of the co-ordinating moieties in stabilizing the nickel(II) complex ion.

The nickel(III) complex may be generated by oxidation with $S_2O_8^{2-}$ in neutral aqueous media. The nickel(III) complex formed initially undergoes speciation to two other complexes with, at best, only very small observable changes in the optical spectra. In addition, the nickel(III) species undergo bulk decomposition to unidentified products (evidence suggests the free ligand and Ni^{2+}). This process is relatively slow with a half-life of approximately 1 h. The observation of kinetic stability of an open-chain nickel(III) amine complex is very rare.

Electron Spin Resonance Spectroscopy.—The kinetic instability of the $[NiL^1]^{2+}$ species under acidic conditions limits the range of oxidants and reductants that may be employed in chemical reaction with the complex. Oxidation with $S_2O_8^{2-}$ provided access to an initial nickel(III) complex, as observed by the isotropic ESR signal obtained with a flat cell at ambient temperature [g_1, Fig. 2(*a*)]. However, the initial spectrum changes with time to give two other signals labelled g_2 and g_3 [Fig. 2(*a*)]. The same overall process has been monitored by rapidly quenching the reaction mixture in liquid nitrogen at specified time intervals, giving the more familiar glass spectra [Fig. 2(*b*)]. In this sequence, an initial isotropic spectrum is formed which is similar to that observed for other NiN_6^{3+} ions. However, further reaction generates a spectrum that is consistent with conversion to an axial species, resembling those formed for $NiN_4X_2^{3+}$ (X = axial ligand) species. Addition of chloride to the final reaction mixture results in a splitting of the axial component but does not fully resolve the feature into the seven lines that would be anticipated for the superhyperfine signal of a dichloride product.

The initial reaction to yield g_1 was sufficiently fast that a stopped-flow ESR technique was employed to monitor the oxidation (Fig. 3). The growth of signal intensity for the g_1 feature as a function of time exhibited first-order behaviour over an initial time interval of 4 min. Analysis of the first-order plots for the formation of g_1 gave a rate constant of $(10.4 \pm 1.5) \times 10^{-3}$ s^{-1} which results in a second-order rate constant of 0.26 ± 0.05 dm^3 mol^{-1} s^{-1}.

By use of time variation of the ESR signals, g_1, g_2 and g_3, it was observed that interconversion and decomposition of the nickel(III) complex $[NiL^1]^{3+}$ takes place. The variation in signal intensities is consistent with further reactions $g_1 \longrightarrow g_2$ and $g_2 \longrightarrow g_3$ which occur with approximate rate constants of 2×10^{-3} s^{-1} and 2×10^{-4} s^{-1} respectively, in 0.8 mol dm^{-3} Li_2SO_4. The conversion of g_2 to g_3 may be monitored by the decrease in the amplitude of the former (Fig. 4). Although the earlier portion of this reaction displays an 'isosbestic' point, indicative of a single process, it is seen that the growth in the signal g_3 rises to a maximum prior to decaying to zero (Fig. 5).

Since, based upon the quenching experiments, the initial nickel(III) species is presumed to convert to a tetragonally distorted octahedral complex, g_2 and g_3 most likely represent differing forms of the octahedral complex. Displacement of

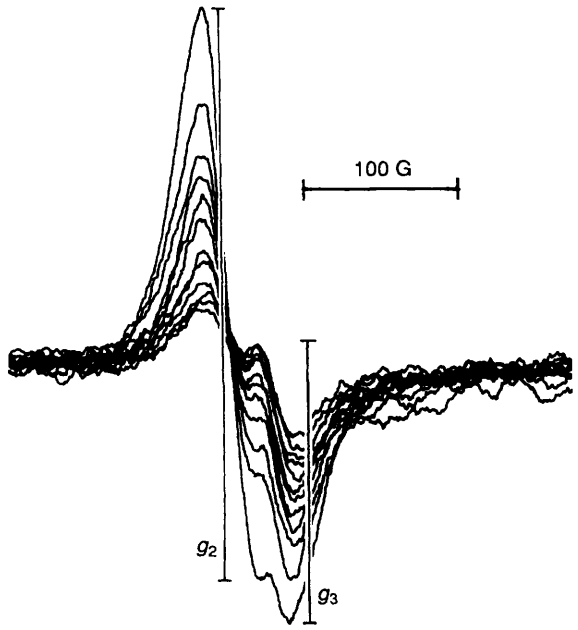

Fig. 4 ESR spectra illustrating the conversion of the isotropic g_2 signal to the isotropic g_3 signal and the overall decay in the intensity of the nickel(III) species

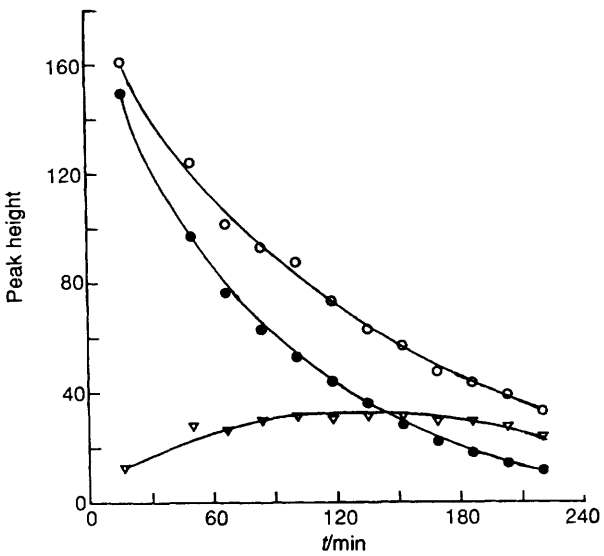

Fig. 5 Graphical presentation of the decay in overall peak intensity (○), g_2 (●) and the appearance and decay of g_3 (▽)

sulfate bound to the metal centre may be forced with an excess of Cl^- (Fig. 2) giving a mixture of the mono- and di-chloride complexes. Thus, g_1, g_2 and g_3 represent the species $[NiL^1]^{3+}$, $[NiL^1(SO_4)]^+$ and $[NiL^1(SO_4)_2]^-$. The structural geometry of the ion suggests that the sulfate ions are monodentate with the remaining co-ordination sites occupied by L^1. Both the mono- and bis-sulfate complexes undergo a reaction resulting in loss of the overall nickel(III) signal intensity (Fig. 5). A rate constant of $(1.3 \pm 0.2) \times 10^{-4}$ s^{-1} may be ascribed to this overall decomposition (Scheme 1), which compares favourably with that obtained from UV/VIS spectroscopy.

Substitution and rearrangement reactions of this type at nickel(III) are rare,[5] since macrocyclic ligands have been used most commonly to stabilize this oxidation state. In such systems, substitution processes are generally inhibited by the inherent strain associated with displacement of the macrocycle. It is also of interest that such processes may be observed only

Table 5 Rate constants for the initial oxidation of $[NiL^1]^{2+}$ with $S_2O_8^{2-}$

Method	$10^3[S_2O_8^{2-}]$/mol dm^{-3}	10^3k_{obs}/s^{-1}
UV/VIS	1	0.4 ± 0.2
	2	0.9 ± 0.2
	5	4.0 ± 0.1
	10	7.3 ± 0.1
	20	11.3 ± 0.1
ESR	20	10.4 ± 1.5
Stopped-flow	5	4.0 ± 0.1
	15	6.7 ± 0.1
	25	15.7 ± 0.1

In all cases, $[NiL^{3\,2+}] = (0.5–2) \times 10^{-4}$ mol dm^{-3}, $T = 20 \pm 1$ °C, $I = 0.1–0.8$ mol dm^{-3} Li_2SO_4.

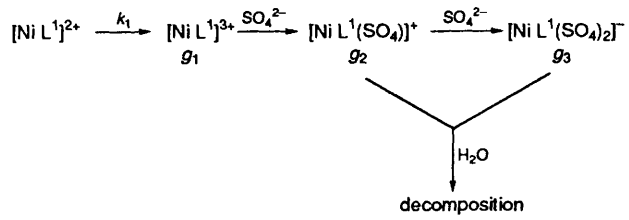

Scheme 1

by use of ESR spectroscopy, the attendant changes in optical density being too small to be detected.

Kinetics.—The kinetics of the oxidation of $[NiL^1]^{2+}$ by $S_2O_8^{2-}$ was investigated by UV/VIS spectroscopy. The resulting reaction profiles exhibit biphasic behaviour with a slow decrease in optical density following a $S_2O_8^{2-}$ dependent increase. This behaviour is consistent with the ESR data. Monitoring the long term decrease in optical density gives a $[S_2O_8^{2-}]$ independent rate constant of $(1.5 \pm 0.15) \times 10^{-4}$ s^{-1}, similar to the rate of decrease in the overall ESR signal intensity. Hence, it is apparent that the UV/VIS spectrometer follows the appearance and disappearance of the nickel(III) ion, regardless of co-ordination geometry.

The initial reaction rates were calculated from the data by compensating for the second process.[20] The data are presented in Table 5. The rate of oxidation of the nickel(II) species by $S_2O_8^{2-}$ is first order in both $[Ni^{II}]$ and $[S_2O_8^{2-}]$, suggesting a simple mechanism for the oxidation of the nickel(II) species with a second-order rate constant of 0.30 ± 0.05 dm^3 mol^{-1} s^{-1}, in excellent agreement with the value obtained by ESR measurement. However, the possibility of ion pair formation with $S_2O_8^{2-}$ prior to oxidation is not precluded nor is the formation of a SO_4^{2-} ion pair. It is the latter possibility that is envisaged as providing the necessary stabilization of the nickel(II) complex and permitting the formation of the nickel(III) complex ion. The hydrogen atoms of the primary amines are oriented 'axially' about the pseudo-C_3 axis of the molecule at an interatomic distance of ≈ 2.5 Å. They are located ideally to form a hydrogen-bonded cap utilizing the sulfate ion of the supporting electrolyte. Such a sulfate ion would then be in position to substitute more readily into the inner co-ordination sphere of the nickel(III) ion.

The reaction was also examined using stopped-flow techniques although the long time base involved presented some difficulties, particularly with respect to separating the two rate constants involved. Thoroughly consistent values were not obtained by analysis of the data as a complete spectral set, using a wavelength range of 280–480 nm. Anomalous behaviour was observed both during the initial 30 s of the reaction and at low wavelengths (< 350 nm). These phenomena may be attributable to the incident light intensity which may result in photolytic

processes occurring within the solution. Indeed, the presence of these processes may have contributed to the overall poor fit observed (Table 5) for the stopped-flow data relative to the UV/VIS and ESR measured rate constants.

It would be of interest to ascertain the self-exchange parameters for the $[NiL^1]^{2+/3+}$ couple. However, owing to uncertainties in the self-exchange rate for the $S_2O_8^{2-}/SO_4^{-}$ SO_4^{2-} system[21] and for the overall driving force for the one-electron process, a Marcus-type correlation is not warranted. A preliminary calculation led to an unrealistically high value ($k_{11} \approx 3 \times 10^{10}$ dm^3 mol^{-1} s^{-1}) for the Ni^{II}–Ni^{III} rate constant. In view of the relatively high redox potential for the $[NiL^1]^{2+/3+}$ couple, the range of reagents available for a detailed investigation of this system is limited. A further consideration is the instability in acidic media of the $[NiL^1]^{2+}$ ion and the overall instability of the $[NiL^1]^{3+}$ complex, which limits the reagents available.

Acknowledgements

We thank Natural Sciences and Engineering Research Council (NSERC) (Canada) and the University of Victoria for the continued financial support of this research, and the former for the funds to purchase a Varian Cary 5 Spectraphotometer and Applied Photophysics DX17MV Stopped Flow instrument.

References

1 M. P. Suh, W. Shin, D. Kim and S. Kim, *Inorg. Chem.*, 1984, **23**, 618.
2 (*a*) I. I. Creaser, A. M. Sargeson and A. W. Zanella, *Inorg. Chem.*, 1983, **22**, 4022; (*b*) R. V. Dubs, L. R. Gahan and A. M. Sargeson, *Inorg. Chem.*, 1983, **22**, 2523; (*c*) P. Bernhard and A. M. Sargeson, *Inorg. Chem.*, 1987, **26**, 4122; (*d*) A. M. Sargeson, personal communication.
3 G. A. Melson, (Editor), *Coordination Chemistry of Macrocyclic Compounds*, Plenum, New York, 1979; L. F. Lindoy, *The Chemistry of Macrocyclic Ligand Complexes*, Cambridge University Press, Cambridge, 1989; J. M. Lehn, *Acc. Chem. Res..*, 1978, **11**, 49.
4 G. W. Bushnell, D. G. Fortier and A. McAuley, *Inorg. Chem.*, 1988, **27**, 2626; S. Chandrasekhar and A. McAuley, *Inorg. Chem.*, 1992, **31**, 2234.
5 E. J. Subak, jun., V. M. Loyola and D. W. Margerum, *Inorg. Chem.*, 1985, **24**, 4350; T. L. Pappenhagen, W. R. Kennedy, C. P. Bowers and D. W. Margerum, *Inorg. Chem.*, 1985, **24**, 4356.
6 J. Lati and D. Meyerstein, *Inorg. Chem.*, 1972, **11**, 2393, 2397; J. Lati, J. Koresh and D. Meyerstein, *Chem. Phys. Lett.*, 1975, **33**, 286.
7 R. W. Green, K. W. Catchpolem, A. T. Phillips and F. Lyons, *Inorg. Chem.*, 1963, **2**, 597.
8 J. E. Sarneski and F. L. Urbach, *J. Am. Chem. Soc.*, 1971, **93**, 884.
9 K. Tomioka, U. Sakaguchi and H. Yoneda, *Inorg. Chem.*, 1984, **23**, 2863.
10 R. J. Geue and G. H. Searle, *Aust. J. Chem.*, 1983, **36**, 927.
11 G. M. Sheldrick, SHELX 76, A Program for Crystal Structure Refinement, University of Cambridge, Cambridge, 1976.
12 P. Coppens, L. Lieserowitz and D. Rabinovich, modified by G. W. Bushnell, University of Victoria.
13 *International Tables for X-Ray Crystallography*, Kynoch Press, Birmingham, 1974, vol. 4.
14 A. McAuley, K. Beveridge, S. Subramanian and T. W. Whitcombe, *Can. J. Chem.*, 1989, **67**, 1657.
15 C. K. Johnson, ORTEP, Report ORNL-5138, Oak Ridge National Laboratory, Oak Ridge, TN, 1976.
16 A. McAuley, S. Subramanian and T. W. Whitcombe, *Can. J. Chem.*, 1989, **67**, 1650.
17 P. Comba, A. M. Sargeson, L. M. Engelhardt, J. M. Harrowfield, A. H. White, E. Horn and M. R. Snow, *Inorg. Chem.*, 1985, **24**, 2327.
18 A. McAuley, P. R. Norman and O. Olubyide, *Inorg. Chem.*, 1984, **23**, 1938.
19 A. McAuley, D. H. Macartney and T. Oswald, *J. Chem. Soc., Chem. Commun.*, 1982, 274.
20 R. G. Wilkins, *The Study of Kinetics and Mechanism of Reactions of Transition Metal Complexes*, Allyn and Bacon, Boston, 1974.
21 U. Fürholz and A. Haim, *Inorg. Chem.*, 1987, **26**, 3243.

Received 26*th January* 1993; *Paper* 3/00498H